

Friction of low-dimensional nanomaterial systems

Wanlin GUO*, Jun YIN, Hu QIU, Yufeng GUO, Hongrong WU, Minmin XUE

Key Laboratory for Intelligent Nano Materials and Devices of the Ministry of Education, State Key Laboratory of Mechanics and Control of Mechanical Structures, and Institute of Nanoscience, Nanjing University of Aeronautics and Astronautics, 29 Yudao Street, Nanjing 210016, China

Received: 22 July 2014 / Revised: 28 August 2014 / Accepted: 30 August 2014

© The author(s) 2014. This article is published with open access at Springerlink.com

Abstract: When material dimensions are reduced to the nanoscale, exceptional physical mechanics properties can be obtained that differ significantly from the corresponding bulk materials. Here we review the physical mechanics of the friction of low-dimensional nanomaterials, including zero-dimensional nanoparticles, one-dimensional multiwalled nanotubes and nanowires, and two-dimensional nanomaterials—such as graphene, hexagonal boron nitride (*h*-BN), and transition-metal dichalcogenides—as well as topological insulators. Nanoparticles between solid surfaces can serve as rolling and sliding lubrication, while the interlayer friction of multiwalled nanotubes can be ultralow or significantly high and sensitive to interwall spacing and chirality matching, as well as the tube materials. The interwall friction can be several orders of magnitude higher in binary polarized *h*-BN tubes than in carbon nanotubes mainly because of wall buckling. Furthermore, current extensive studies on two-dimensional nanomaterials are comprehensively reviewed herein. In contrast to their bulk materials that serve as traditional dry lubricants (e.g., graphite, bulk *h*-BN, and MoS₂), large-area high-quality monolayered two-dimensional nanomaterials can serve as single-atom-thick coatings that minimize friction and wear. In addition, by appropriately tuning the surface properties, these materials have shown great promise for creating energy-efficient self-powered electro-opto-magneto-mechanical nanosystems. State-of-the-art experimental and theoretical methods to characterize friction in nanomaterials are also introduced.

Keywords: friction; nanomaterials; two-dimensional materials; nanotubes; nanoparticles; energy dissipation

1 Introduction

Friction is the force that resists the relative motion of solid surfaces, fluid layers, and material elements that slide against each other and arises from interatomic forces between the two surfaces in contact. To maintain motion, energy barriers must be overcome, in the process of which some kinetic energy is inevitably converted into thermal energy, which results in energy dissipation. In fact, friction accounts for about one-third of the world's energy consumption [1]. For example, humans use about 360 million tons of oil per year worldwide to overcome friction in passenger cars [2]. Besides energy dissipation, many types of friction also

cause the removal of material from either or both contacting surfaces; this phenomenon is referred to as “wear”. Friction and wear significantly decrease the performance and lifetime of mechanical equipment and thus cause huge economic loss in industrial activities. Fortunately, much progress has been made by scientists and engineers over the past century to better understand and control both friction and wear, thus gradually decreasing energy and economic loss. In fact, both friction and wear may be minimized by careful modification of the surface properties of the surfaces in contact or by using lubricating films between the surfaces in contact.

The classical concepts of friction were established in the 15th to 18th centuries, mainly by da Vinci, Amontons, and Coulomb. The first research leading

* Corresponding author: Wanlin GUO.
E-mail: wlguo@nuaa.edu.cn

to the classical rules of sliding friction dates back to the 15th century and was done by Leonardo da Vinci, who realized the importance of friction between moving parts of mechanical systems and noted that contact area had no effect on the friction properties [3]. In the 18th century, Amontons and Coulomb proposed the classical friction equation that describes sliding friction and determined the factors that affect friction properties such as the type of material and the surface coatings [4]. Coulomb also made the distinction between static and kinetic friction [4]: For kinetic friction, the surfaces in contact move relative to each other whereas, for static friction, the surfaces remain relatively static with respect to each other. In the late 18th century, Reynold derived the equation of viscous flow that describes the mechanics of a lubricating fluid film. From this equation was built the three classical friction models (static, kinetic, and fluid) that are currently in wide use in industrial activities have been established. The three classical laws of friction may be summarized as followed based on macroscopic experiments [3]: (i) Friction is independent of the apparent area of contact; (ii) friction increases proportionally to the applied load; and (iii) kinetic friction is independent of the sliding velocity. These classical laws of friction continue to play important roles in modern mechanical engineering and in manufacturing (e.g., to improve the reliability and lifetime of equipment). However, research into friction on the macroscopic scale cannot explicitly consider the influence of the microscopic structures and properties, so large limitations arise when the classical friction laws are applied directly to friction on the micro- or nanoscale. For example, in 1950, Bowden and Tabor found that the true contact area is formed by the asperities and is smaller than the apparent contact area [5].

Since the late 20th century, the rapid development in nanoscience and nanotechnology has provided a fascinating opportunity to investigate friction on the nanometer scale. In fact, friction and wear depend strongly on the surfaces of the solids in contact, and the macroscopic properties of these surfaces are sensitive to their atomic and molecular structure. In addition, friction may also change the microstructure of the surfaces in contact, in particular under high lateral load or after long-term working. To better

understand these micro- or nanoscale mechanisms of friction requires a revolution in experimental and computational friction-research tools. The invention of scanning probe microscopies [6], including scanning tunneling microscopy (STM), atomic force microscopy (AFM), friction-force microscopy (FFM), and lateral-force microscopy (LFM), together with specific friction-research equipments such as surface-force apparatus and quartz crystal microbalances, have allowed scientists to investigate experimentally atomic-scale friction and interface characteristics at high resolution and to propose schemes to precisely control the surface properties of nanoscale structures [7]. In addition to experiment, theoretical modeling plays an important role in understanding friction mechanisms on the atomic- and nanoscale. For example, a pioneering attempt to explain friction on the atomic level was made by Tomlinson [8] in 1929. He considered surface atoms as single independent oscillators that are “plucked” by the atoms of the opposite surface like a guitar string; in other words, they are independent oscillators connected to a sliding surface in a fixed potential that describes the opposite surface. Another typical model for taking into account the coupling between atoms is the Frenkel–Kontorova model [9], which models a monolayer adsorbed onto an atomically flat surface. It is a one-dimensional model with a chain of adsorbate atoms coupled linearly by nearest-neighbor interactions. The chain interacts with a spatially periodic potential. Later, a mechanical model called the Frenkel–Kontorova–Tomlinson model [10] was established, which combines the Frenkel–Kontorova model with the Tomlinson model by coupling each atom harmonically to the sliding body. In addition, the rapid growth in computational techniques such as molecular dynamics simulations [11] offers a chance to understand the nanoscale mechanisms behind tip-surface frictional interactions. Using these theoretical models and experimental and computational tools, many researchers have focused on the physical mechanics of friction on the molecular and atomic scales to connect the friction properties of materials to their microstructure [12]. Research into the physical mechanics of friction has become more important now, in particular when multifield coupling between force, electric and magnetic fields, and



temperature and humidity have to be considered to understand friction on the nanoscale.

The materials involved in friction, especially in lubrication, have also been the subject of significant development over the past century. For instance, for brake systems, multiphase composites have been developed to provide stable and reliable friction coefficients and low wear over a wide range of working conditions [13, 14]. In addition, lubricating materials have been widely used to minimize friction between surfaces in contact. Conventional lubricating materials include oil, water, grease, as well as layered materials such as graphite, hexagonal boron nitride (*h*-BN), and transition-metal dichalcogenides. With the development of nanotechnology, a variety of novel low-dimensional nanomaterials have been found to have exceptional lubricating properties. In fact, the friction properties of nanomaterials have become ever more important in nanotechnology, and intriguingly, most traditional dry lubricating materials are being transformed into highly attractive functional nanomaterials, such as graphene (a single layer of graphite), monolayer *h*-BN, and transition-metal dichalcogenides. Actually, these monolayered materials constitute the core members of the current hottest two-dimensional (2D) nanomaterial family in the world. The topological insulators emerging from fundamental physics are in fact layered materials that have also long been used as lubricants.

In this review, we provide a comprehensive discussion of the advances in friction research on such low-dimensional nanomaterials and of the interplay between friction, atomic structure, and physical properties. We start with a brief review of friction in zero-dimensional (0D) materials (i.e., nanoparticles and balls with no dimensions greater than the nanoscale) then discuss one-dimensional (1D) nanomaterials such as nanotubes and nanowires, in which one dimension is greater than the nanoscale, and finally discuss 2D nanomaterials, which are macro-size in a plane but are one or several atoms thick.

2 Friction in zero-dimensional nanomaterials

Ball bearings are an important way to reduce rolling friction, but when the balls become nanoscale in size,

their role changes significantly. Zero-dimensional nanoparticles are ultrafine particles with diameters ranging from 1 to 100 nanometers. Due to their exceptionally large surface area and their small size, nanoparticles exhibit quite different physical and mechanical properties compared with their bulk and micro-scale counterparts. These properties make them ideal for improving the tribological properties of lubricants and the performance of composite coatings [15]. Interactions between nanoparticles or between nanoparticles and a surface arise from the diverse interaction forces that occur, including van der Waals, electrostatic, capillary, solvation, hydration, etc. [15]. The rolling and sliding movement of nanoparticles in lubrication could provide low friction and wear [12], which play important roles in nanofabrication, lubrication, drug delivery, and the design of nano-devices. Because empirical theories are hard pressed to explain these nanoscale tribological properties of nanoparticles, researchers have renewed efforts to establish the main factors that determine nanoscale friction. In fact, nanoscale friction has been studied extensively ever since it was first detected with AFM by Mate et al. [16]. In other work, Dietzel et al. found that two frictional states coexist during nanoparticle sliding: The friction of some particles increases linearly with contact area, whereas others experience frictionless sliding [17]. Tevet et al. explored the friction mechanism of fullerene-like nanoparticles with high-resolution transmission electron microscopy (TEM; see results in Fig. 1) [18]. The three main mechanisms causing friction for nanoparticles are rolling, sliding, and exfoliation, and low friction and wear may be achieved with these fullerene-like nanoparticles by improving their sphericity, dispersion (de-agglomeration), and the smoothness of the mating surfaces. Strong friction anisotropy is found when the two-fold surface of an atomically clean aluminum-nickel-cobalt quasicrystal slides against a thiol-passivated titanium-nitride tip. These results indicate a strong connection between surface atomic structure and the mechanisms that dissipate energy, which likely include electronic and/or phononic contributions [19]. Dietzel et al. studied the transition from static to kinetic friction for metallic nanoparticles and found that the hysteretic character in the force domain is characterized by a constant

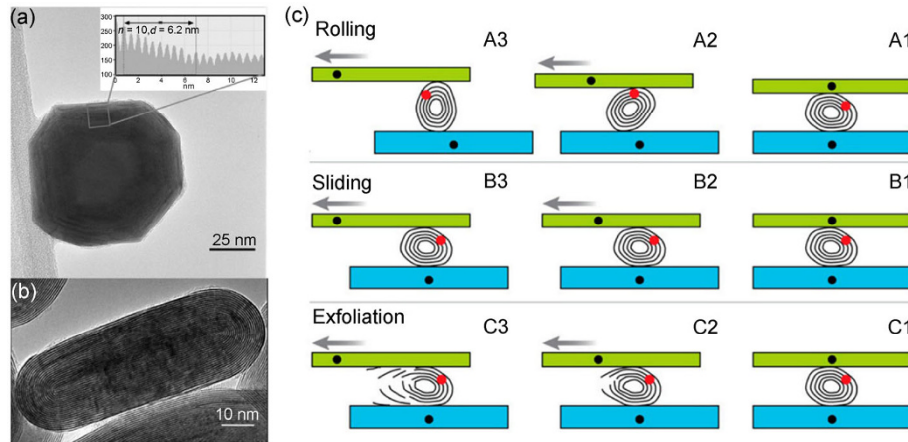


Fig. 1 TEM images of a typical hollow multilayered fullerene-like WS_2 nanoparticles (a) and fullerene-like MoS_2 nanoparticles (b). The line profile of the boxed area gives an interlayer spacing of 6.20 Å. (c) Three main friction mechanisms of multilayered nanoparticle: rolling (A1–A3), sliding (B1–B3), and exfoliation (C1–C3). The bottom surface is stationary while the upper surface is moving to the left. The red mark is a point of reference, i.e., gold nanoparticle in the experiments [18].

kinetic-to-static-friction ratio of 0.5 [20]. Furthermore, the friction and wear properties of surface-modified TiO_2 nanoparticles [21], alumina nanoparticles filled with polytetrafluoroethylene (PTFE) [22], hollow inorganic fullerene-like MoS_2 nanoparticles [23], and thin films of fullerene-like MoS_2 nanoparticles [24] were also investigated for potential applications in nanofabrication and lubrication.

3 Friction in one-dimensional nanotubes and nanowires

One-dimensional carbon nanotubes have a constrained geometry, small interlayer distance, wear-free interlayer sliding, and ultralow friction. These features make them ideal building blocks for fabricating nanofunctional mechanical devices. Cumings et al. [25, 26] created linear bearings out of multiwalled carbon nanotubes (MWCNTs; see Fig. 2). The interlayer telescoping friction force in the MWCNTs was estimated to be less than 1.5×10^{-14} N per atom. Fennimore et al. [27] created a rotational actuator by using a MWCNT as the motion-enabling element. Zheng and colleagues [28, 29] proposed that MWCNTs be used to create gigahertz nano-oscillators. When both ends of the outer shell are opened, the retracted core will not stop at its original position but will oscillate with respect to the outer housing at gigahertz frequency, in accordance with conservation of energy. Since the principles of

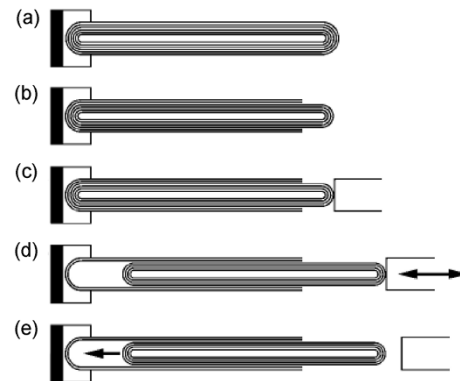


Fig. 2 Schematic representation of the experiments performed inside TEM. The process of opening the end of a MWCNT (a), exposing the core tubes (b), and attaching the nanomanipulator to the core tubes (c). (d) and (e) Two different classes of subsequent experiments performed. (d) The nanotube is repeatedly telescoped while observations for wear are performed. (e) The core is released and pulled into the outer shell housing by the attractive van der Waals force [25].

carbon nanotube nano-oscillators were elucidated, many MWCNT mechanical devices have been designed, but successful experimental implementation and observation are rare. A fundamental problem for these devices is to maintain the mechanical motion for sufficiently long or, in other words, to minimize the rate at which their mechanical energy is dissipated as heat.

To address these problems of energy dissipation and friction in carbon-nanotube mechanical system, Guo et al. [30] used atomistic models and molecular

dynamics simulations to investigate energy dissipation, interlayer-corrugation effects, and resistance force in (10,10)/(5,5), (18,0)/(5,5), and (18,0)/(9,0) biwalled carbon nanotubes. They found that significant energy is dissipated in all nanotube systems, although the energy dissipated by (10,10)/(5,5) bitube oscillators is much greater than that dissipated by (18,0)/(5,5) oscillators, as shown in Fig. 3. This result means the oscillation amplitude decays within a few nanoseconds for the (10,10)/(5,5) bitube and within several tens of nanoseconds for the (18,0)/(5,5) bitube. In addition to

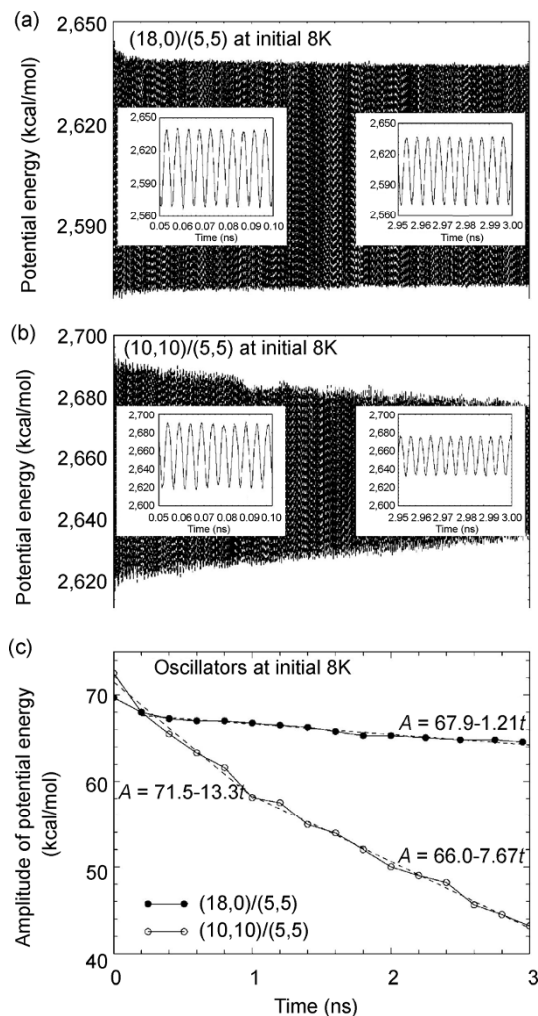


Fig. 3 Variation of potential energy with time at an initial temperature of about 8 K. (a) (18, 0)/(5, 5) tube system; (b) (10, 10)/(5, 5) tube system; the insets show variation of potential energy around 50 and 3,000 ps. (c) Reduction of amplitude of potential energy with oscillating time. The tube length is about 3 nm and the initial extrusion displacement is about 1/4 of the tube length. The dashed linear lines and equations in (c) are corresponding fitting curves of the molecular dynamic simulation results [30].

the effects due to the interlayer arrangement, theoretical studies indicated that the excitation of phonons (due to the interaction of the carbon-nanotube core with the edge of the outer casing) and thermal fluctuations could be mechanical sources of energy dissipation. For example, Zhao et al. [31] studied energy transfer from the translational degrees of freedom to phonon modes for two coaxial carbon nanotubes. They found that, for oscillators with short nanotubes, a rocking motion, occurring when the inner tube is pulled about a third of the way out of the outer tube, is responsible for significant transfer of energy to phonons. For oscillators made from long nanotubes, translational energy is mainly dissipated via a wavy deformation in the outer tube as it undergoes radial vibrations. Servantie and Gaspard [32] developed theoretical and numerical methods to calculate the dynamic friction coefficient based on an adiabatic approximation that uses the temporal integral of the autocorrelation function of the force between both sliding objects. They used these methods to evaluate the kinetic-friction coefficient for the relative motion of two concentric carbon nanotubes and found that it increases with temperature. By using molecular dynamics simulations, Legoas et al. [33] studied the telescopic extension and retraction motion of MWCNT nano-oscillators and revealed that, independent of tube type, sustained oscillations are possible only when the radii of the inner and outer tubes differ by $\sim 3.4 \text{ \AA}$. Rivera et al. [34] used molecular dynamics simulations to study the oscillatory motion of incommensurate and commensurate double-walled carbon nanotubes (DWCNTs) that result from the pull-out of the inner nanotube before releasing it. They concluded that the oscillations in DWCNTs are damped and that the system acts as a nanosized shock absorber. Furthermore, they attributed the frictional forces between nanotube surfaces to thermal fluctuations in the nanotube conformation. Other theoretical simulations and models revealed that thermal-induced edge barriers and forces can govern the interlayer friction of DWCNTs [35], and energy dissipation in MWCNTs coming from phonons excited by the interaction of the core with the edge of the outer casing [36]. Further studies on interaction forces leading to energy dissipation in MWCNTs showed that the interlayer resistance can vary with tube morphology, length, and diameter. In a commensurate

pair of tubes, the fluctuation of interlayer sliding-resistance force increases with tube length, but in an incommensurate pair this force can remain unchanged [37]. Recent experiments conducted by Zhang et al. [38] show that, under ambient conditions, superlubricity can occur in centimeter-long DWCNTs with perfect structures. Here, intershell friction was measured while the inner shells were pulled out from centimeter-long DWCNTs. The intershell friction was nearly independent of pull-out length and could be as low as 1 nN, as shown in Fig. 4. The shear strength of the DWCNTs was only several Pascals. Superlubricity in DWCNTs can be understood in terms of the absence of defects and the large axial curvature in the DWCNTs, as well as the length-independent variation of the van der Waals interaction between the CNT shells as they are being pulled apart. These researches and progress in interlayer interaction, friction, and energy dissipation between carbon nanotubes provide significant insights into the design of nanotube-based devices.

In most cases, various topological defects such as vacancies, Stone–Wales defects, and adatoms are hard to avoid during MWCNT growth, and this might lead to energy dissipation during intershell sliding in MWCNTs. Guo et al. [40] used molecular statics and dynamics simulations to study interlayer friction and energy dissipation in biwalled carbon nanotubes of different chirality and size, and with and without defects. In incommensurate systems at very low temperature, the interlayer friction force of a perfect bitube system was found to strongly depend on commensuration and to be independent of tube length. However, the existence of defects can ruin the perfect-geometry controlled interlayer interaction, thereby leading to a sharp increase in friction and energy dissipation. These theoretical calculations of Stone–Wales defects on a core interacting with the open end of the casing or of such defects on the casing interacting with the capped core are consistent with the amplitude and spatial extent of experimentally measured force fluctuations in the cyclic telescoping motion of MWCNTs [41]. In that experiment, Kis et al. measured interlayer force during prolonged cyclic telescoping motion of a MWCNT. They found that the force acting between the core and the outer casing is modulated by the presence of stable defects and generally exhibits ultralow friction (below the

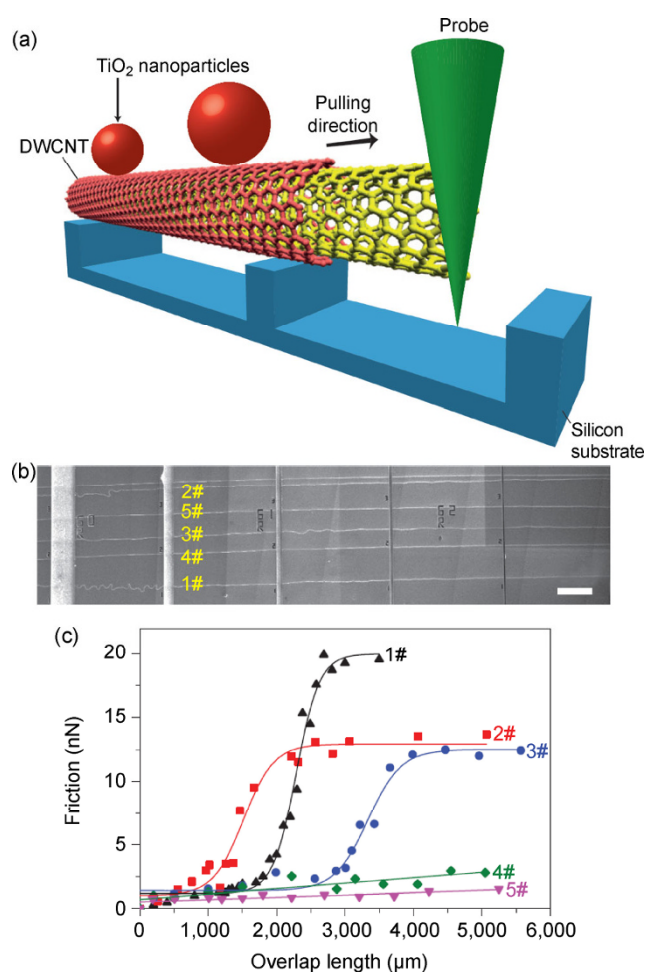


Fig. 4 (a) Schematic of the experiment illustrating a process of pulling out the inner shell (yellow) from its outer host (red) through a sensitive force probe. Contact length between the inner extracted tube and the outer one changes from tens of nanometres to centimetres. The carbon nanotubes were decorated with TiO₂ nanoparticles that enabled efficient manipulation of individual nanotubes. For clarity nanoparticles and nanotubes are not shown to scale [39]. (b) SEM image of ultralong MWCNTs with different axial curvatures. (c) Measured friction for the five ultralong MWCNTs shown in (b). The intershell friction (4# and 5#) was lower than 3 nN when the overlap length was about 5,000 μm or smaller [38].

measurement limit of 1.4×10^{-15} N/atom) and total dissipation per cycle lower than 0.4 meV/atom. They also found that the defects lead to temporary mechanical dissipation.

Boron nitride nanotubes (BNNTs) have a structure similar to that of carbon nanotubes, but with alternating B and N atoms with respect to C atoms in the tube lattice. The properties of interlayer friction in BNNTs are important for their applications in nanomechanics.

Recently, by using a quartz-tuning-fork-based atomic force microscope and a nanomanipulator, Niguès et al. [42] compared the mechanical response of multiwalled carbon nanotubes and multiwalled BNNTs during the fracture and telescopic sliding of the layers, as shown in Fig. 5. They found that the interlayer friction for insulating BNNTs results in ultrahigh viscous-like dissipation that is proportional to the contact area, whereas for the semimetallic carbon nanotubes the sliding friction vanishes (within the experimental uncertainty). They ascribed this difference to the ionic character of the BN, which allows charge localization.

The properties of friction in nanowires have also attracted the interest of scientists. Most research has focused on static and kinetic friction in nanowires together with their elastic properties. Zinc-oxide nanowires and silicon nanowires have been frequently used to probe the mechanical characteristics and mechanisms of friction between one-dimensional nanowires and two-dimensional substrates [39, 43, 44]. Nanowires are generally manipulated by using an AFM or STM probe [45]. In fact, the rolling frictional characteristics and sliding frictional characteristics were observed in a recent study by Kim et al. [46] (see Fig. 6). They claimed that the friction coefficients

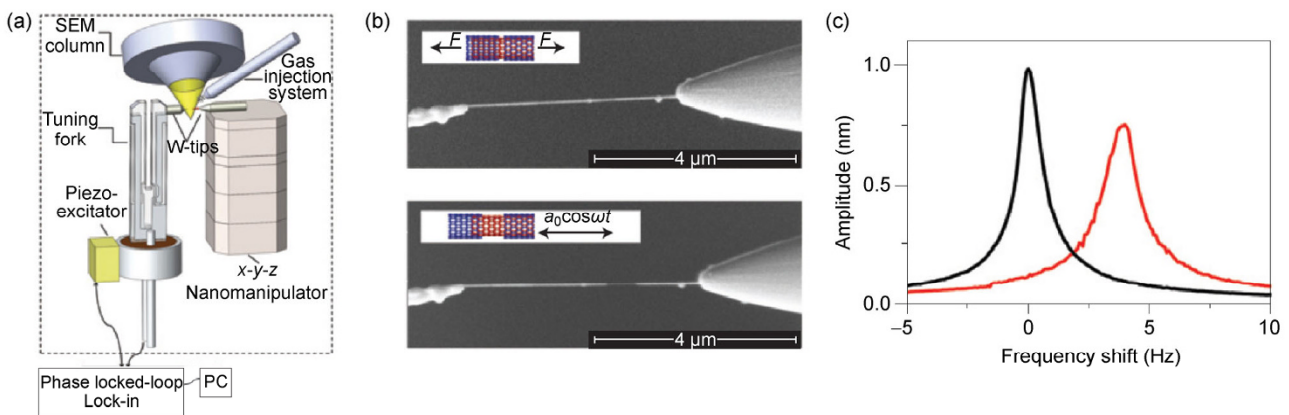


Fig. 5 Multiwalled nanotube Christmas-cracker experimental set-up. (a) Schematic drawing of the experiments, showing a multiwalled nanotube assembled to a tuning-fork on one side, and to a nanomanipulator on the other side. A piezo system excites the oscillator at the resonance frequency (≈ 32 kHz); a lock-in and a phase-locked loop maintain both the amplitude and the phase constant between the tuning fork and the excitator. (b) SEM images of a carbon nanotube glued to each tungsten tip during the tensile experiments. Nanotube has a length of $5.5 \mu\text{m}$, external diameter of 60 nm and sliding tube diameter 25 nm . (c) Amplitude resonance curves for both free and interacting tuning forks. The black curve represents the free resonator oscillating in vacuum with a quality factor $Q = 45,000$. The red curve represents the tuning-fork response during telescopic intershell sliding with a quality factor $Q = 18,000$ [42].

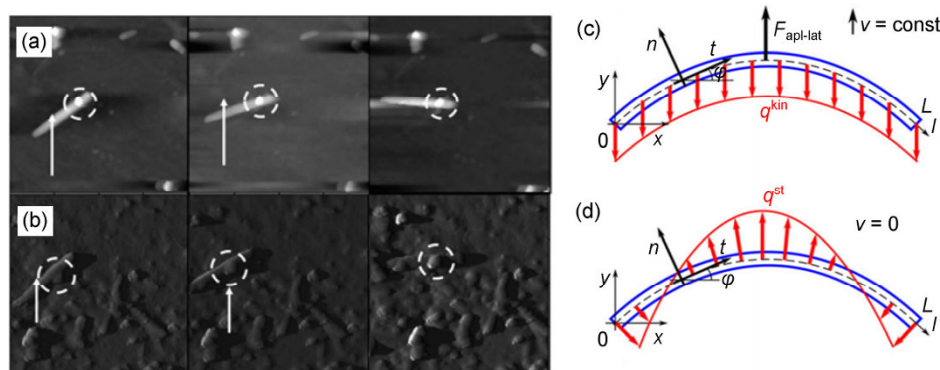


Fig. 6 AFM images of ZnO nanowires translation motion during manipulation for the case of (a) pure sliding and (b) both rolling and sliding. Dotted circle is the marker for the translation motion [46]. Schematics of a bent nanowire affected by (c) kinetic friction force and (d) distributed static friction force [48].

were similar to those of macroscale systems once adhesion was considered. Static friction between silicon nanowires and elastomeric substrates was studied by Qin and Zhu, who found that frictional characteristics were sensitive to the substrate treatment [47]. A model of kinetic and static friction between an elastically bent nanowire and a flat surface was proposed by Romanov et al. [48], who considered two cases as the fundamental situation for studying kinetic and static frictions.

4 Frictional properties of two-dimensional layered materials.

Two-dimensional materials have attracted extensive research interest since the electronic properties of mechanically exfoliated monolayer graphene were first revealed in 2004 [49]. Compared to the 0D and 1D materials reviewed above, the planar structure makes them much easier to incorporate into modern industry, which requires precise control and manipulation of the target. For practical applications, especially in micro-electromechanical systems (MEMS) and their nanoscale counterpart nano-electromechanical systems (NEMS), their frictional properties should be thoroughly understood. Actually, the ultralow friction of their bulk counterparts (i.e., layered materials such as graphite, molybdenum disulphide, and boron nitride) make them ideal lubricants in mechanical systems such as aerospace systems, high-vacuum systems, and systems that operate over a wide temperature range [50–52]. This ultralow friction is attributed to the weak interlayer bonding (van der Waals forces) compared with the strong inlayer chemical bonding of layered materials, making them easy to shear. Moreover, because the van der Waals interlayer interaction decreases with increasing temperature, the friction of layered materials can be further reduced at elevated temperature [50, 53].

Generally, the 2D counterparts of these materials inherit their ultralow-friction characteristics. However, due to their special structural dimensionality and excellent mechanical properties, they also exhibit quite different frictional characteristics compared to their bulk counterparts, as has been demonstrated with a variety of experimental and computational methods.

4.1 Dependence of friction on layer number and substrate

Lee et al. [54] undertook the first work concerning the impact on friction characteristics of the number of layers of 2D materials prepared by mechanical exfoliation. They found that the frictional force on graphene exfoliated onto SiO₂/Si substrates increases with decreasing graphene thickness. They attributed this result to an increase in the van der Waals force as the SiN tip approaches the substrate, a conclusion that was confirmed by force spectroscopy measurements. In addition, they found that friction depends logarithmically on velocity, which they attributed to the thermally activated stick-slip effect. Soon afterwards, this dependence on the number of graphene layers was confirmed by Lee et al. for both suspended and supported graphene (see Fig. 7) [55]. They excluded substrate effects, variations in adhesion force, scan rate, and load as possible explanations and proposed instead a rippling-rug effect to explain the results. Their further work concerning 2D materials, including graphene, molybdenum disulfide (MoS₂), niobium diselenide, and hexagonal boron nitride, showed that this trend applies to all materials used in their research that were exfoliated to a weakly adherent substrate (silicon oxide) or suspended from a micron-sized hole [56, 57]. Once the samples were bound strongly to a mica surface, this trend was suppressed. Based on solid experimental evidence and finite-element modeling, they suggested that this trend arises from the increase in the susceptibility of the thinner sheet to out-of-plane elastic deformation. Recently, they went a step further and determined the effect of surface morphology on friction with graphene [58]. These measurements revealed that graphene maintains its corrugation level even after it is refolded onto an atomically flat substrate and that both the graphene and the substrate must be ultraflat to achieve the intimate contact necessary for strong adhesion and low friction.

The interpretation of the observation of Lee et al. was supported by the Brownian dynamics simulations of Smolyanitsky et al. [59] and by the molecular dynamics simulations of Ye et al. [60]. The tip-induced out-of-plane deformation of 2D materials was also experimentally confirmed and systematically studied by Barboza et al. [61]. They referred to this effect as

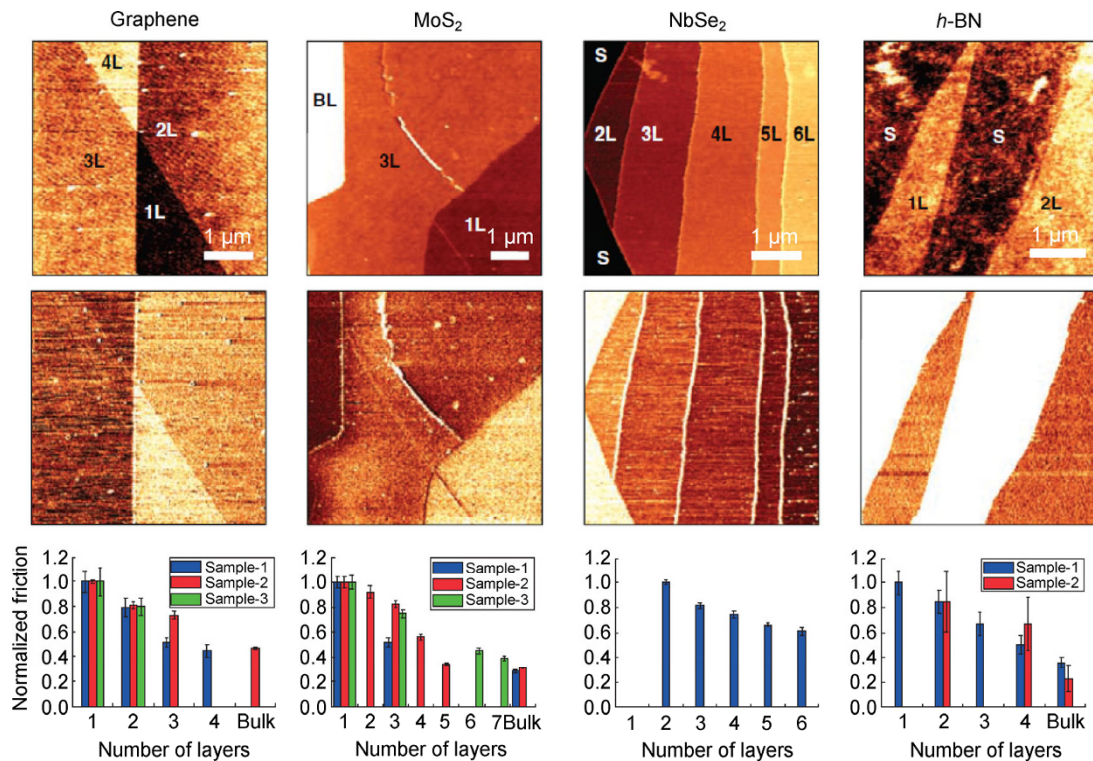


Fig. 7 Dependence of the frictional force on the layer number of graphene, MoS₂, NbSe₂ and h-BN, respectively [55].

“dynamic negative compressibility”: When the probe tip slides on these 2D materials, a vertical expansion proportional to the applied normal load appears for dynamical wrinkling of the upper material layers induced by the simultaneous compression and shear from the tip.

This dependence on layer number is not limited only to mechanically exfoliated samples, but also applies to graphene prepared through chemical vapor deposition, as shown by Egberts et al. [62]. They showed that the friction force of monolayer graphene is significantly larger than that of bilayer graphene deposited on copper foil and proved that layer-dependent friction properties result from puckering of the graphene sheet around the sliding tip, consistent with the model proposed by Lee et al. Furthermore, in the normal force as a function of friction, they observed a substantial hysteresis with repeated scanning without breaking contact with the graphene-covered region. Because of this hysteresis, friction measured on graphene changed as a function of time and maximum applied force. For graphene films grown epitaxially on SiC, the friction on monolayer graphene

was also found to be a factor of two greater than that on bilayer films, as shown in Fig. 8 [63, 64]. However, based on results of angle-resolved photoemission spectroscopy, the difference in friction between single and bilayer graphene is found to arise from a dramatic difference in electron-phonon coupling. Monolayer graphene was found to have a remarkable electron-phonon coupling, which can efficiently dampen lattice vibrations and thus enhance the energy dissipation induced by friction. In bilayer graphene, however, electron-phonon coupling almost vanishes, so friction is reduced as well. In addition, it was demonstrated that, because of reduced adhesion, friction on bilayer graphene epitaxially on SiC is even less than that on graphite. At normal loads of 40 nN, a transition from atomic stick-slip friction to a regime of ultralow friction occurs.

4.2 Frictional characteristics of chemically modified 2D materials

Two-dimensional materials consist of only a single layer of atoms, all of which are exposed to the surface. Thus, most of their properties can be easily tuned

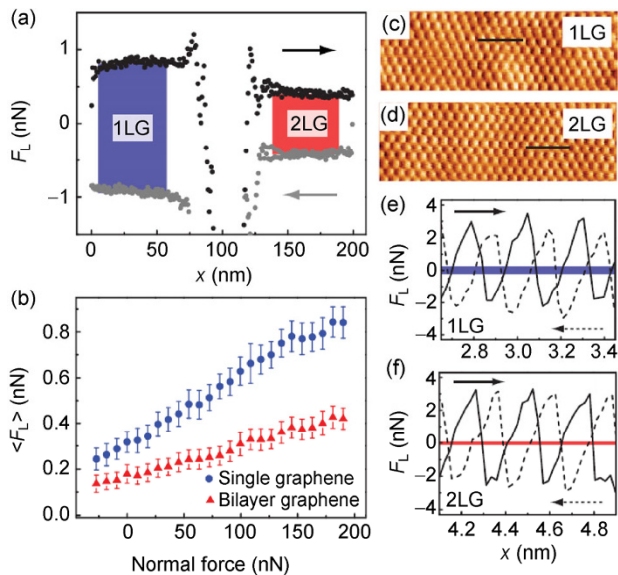


Fig. 8 The friction force on monolayer and bilayer graphene epitaxially grown on SiC [63].

by chemical modification, including their frictional properties. The most-studied chemically modified 2D material is oxidized graphene. Several works of different groups have demonstrated that friction in graphene is notably enhanced by oxidation [65–67]. For this reason, oxidized graphene can easily be distinguished from a graphite surface by lateral-force microscopy [67]. The enhanced friction also holds for graphene-oxide nanoribbons, whose friction can be further increased by exposing it to high humidity [68]. By using density functional theory, Wang et al. investigated the atomic-scale friction in graphene oxide, revealing the atomic origination of the enhanced friction [69]. In addition, an adhesion-dependent

negative friction coefficient was found by Deng et al. on oxygen-modified graphite, as shown in Fig. 9 [70]. They found that, when the adhesion between AFM tip and surface is enhanced by chemisorbed oxygen relative to the exfoliation energy of graphite, friction can increase as the normal load decreases under tip retraction. Based on both atomistic and continuum-based simulations, they attributed this phenomenon to a reversible partial delamination of the few topmost (or single) layers of graphene. During tip retraction, lifting these topmost layers leads to greater deformability of the surface, and thus increases the friction force.

For hydrogenated graphene, the friction force is three times higher than for pristine graphene [65]. However, based on *in situ* cleaning with an AFM tip, Fessler et al. attributed this to surface contamination [71]. Once cleaned, the frictional behavior became the same as for pristine graphene. Kwon et al. showed that the friction of a graphene surface increased six times after surface fluorination, whereas the adhesion force was slightly reduced [72]. Based on density functional theory, they attributed this result to a higher out-of-plane bending stiffness for fluorinated graphene. They also proposed that damping via flexural phonons is a main source of frictional energy dissipation in 2D materials such as graphene.

4.3 Influence of defects on friction of 2D materials

Structural defects, such as edges, grain boundaries, and vacancies, are inevitable in 2D materials prepared by current methods. The presence of these defects

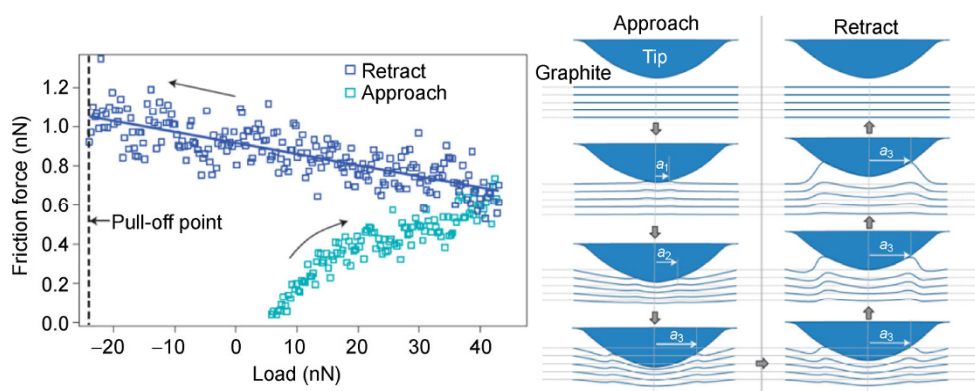


Fig. 9 Adhesion-dependent negative friction coefficient on oxygen modified graphite.

introduces significant modifications in the material properties, especially electronic properties. Some recent works have also investigated the influence of defects on friction in 2D materials. In 2008, friction across the edges of 2D materials (graphene and MoS_2) was found to increase for both step-down and step-up scans [73]. The additional frictional force due to the step edge increases linearly with load for upward jumps, but remains constant for downward jumps. A modified Prandtl–Tomlinson model featuring a Schwoebel–Ehrlich barrier at the steps was proposed by Schwarz et al. to explain this phenomenon (Fig. 10). Following this, Hunley et al. demonstrated that this additional frictional force can be suppressed by a single overlapping layer of graphene. By sliding a sharp tip upward over the exposed step, they also obtained evidence of elastic straining of graphene edges introduced by the tip, demonstrating another possible

contribution to increased friction. Actually, the enhanced friction induced at the edges was also observed for the bulk counterparts of these 2D materials, such as graphite and hexagonal boron nitride. The high-energy edge surface of these bulk materials, although representing a small proportion of the overall surface, increases the adhesion between the opposing surfaces and thus significantly increases the friction [50]. However, because the edge energy could be efficiently reduced by absorbed molecules or by introducing functional groups, the friction coefficient of outgassed graphite and boron nitride was shown to decrease by a factor of three for many different gases [53].

Grain boundaries and vacancies are two types of defects that may also affect friction. Molecular dynamics simulations of a short capped single-walled carbon nanotube sliding on graphene with a vacancy or a Stone–Thrower–Wales defect shows significant change in lateral forces with different characteristics [74]. However, these predicted changes in friction across grain boundaries were not detected by Kwon et al. [75] with friction-force microscopy. A possible reason for this result may be the large size of the probe tip compared to the size of the carbon nanotube used in the simulation. Experiments with carefully prepared probes are required to clarify this problem. Although the influence of grain boundaries on friction remains poorly understood, the friction domains of monolayer graphene supported on SiO_2/Si substrates were observed [76]. By using angle-dependent scanning, Choi et al. observed friction anisotropy with a periodicity of 180° in each friction domain. They attributed the friction domains to the ripple distortions of the graphene, which gives rise to anisotropic friction in each domain as a result of the anisotropic puckering of the graphene.

4.4 Interlayer friction

Theoretical studies based on different models have been conducted to better understand atomic-scale friction between finite and infinite graphene sheets [11, 77]. The interlayer superlubricity state of graphite depends not only on the interlayer interaction but also on the pulling direction and the corresponding registry of each layer. The low friction force and friction coefficient in graphite also depend on loading

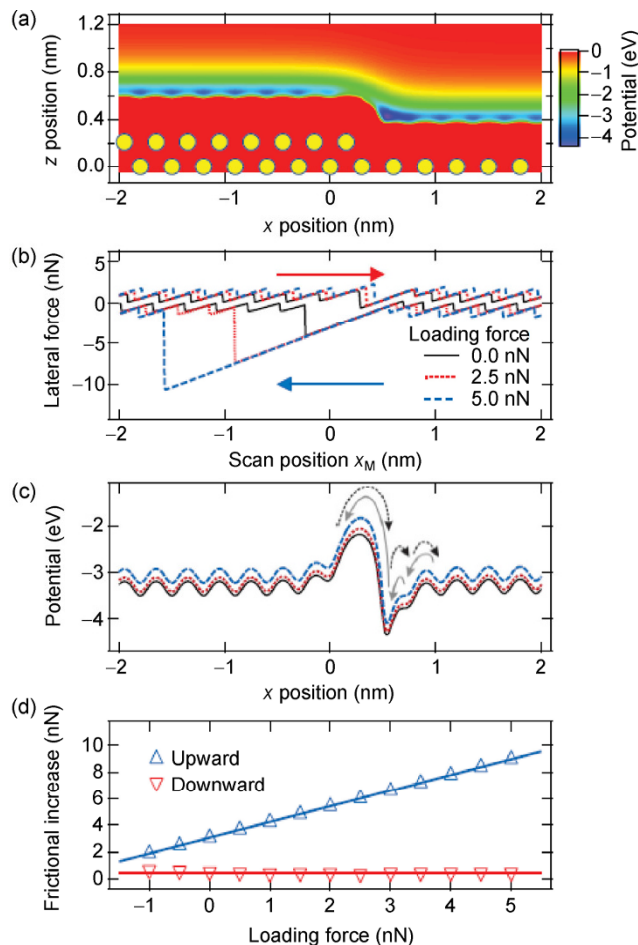


Fig. 10 The origination of the additional frictional force across the steps [73].

force and interlayer stacking structures [11]. Guo et al. [78] studied the effects of changing the interlayer separation and of in-sheet defects on the interlayer friction between graphene sheets (Fig. 11). The interlayer friction between graphene sheets with commensurate or incommensurate interlayer stacking increases with decreasing interlayer separation. The ultralow interlayer friction in incommensurate stacked sheets is insensitive to the in-sheet vacancy defects at certain orientations. Changing interlayer separation and introducing defects may be a way to achieve ultralow friction and control friction properties in graphene sheets. By using a tight-binding atomistic simulation, Bonelli et al. [79] investigated the slipperiness of graphene flakes against a graphite surface and revealed the crucial role of flake rotation in determining the static friction.

4.5 Frictional interaction between liquid and 2D materials

Experiments have shown that the flow rate of water inside carbon nanotubes is unexpectedly high due to

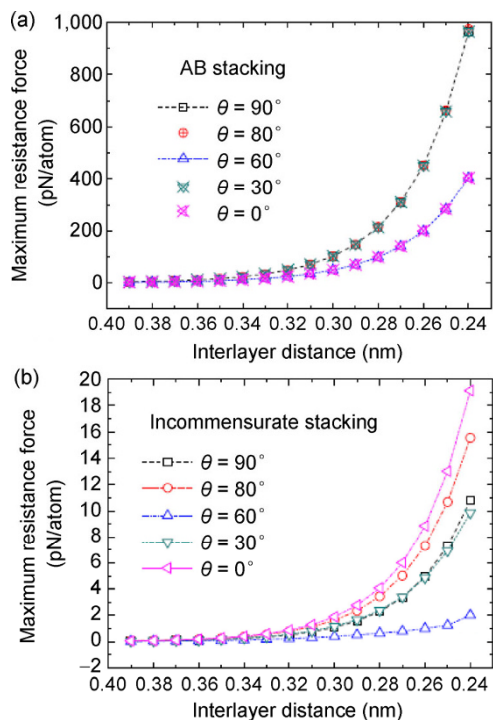


Fig. 11 Maximum resistance force acting on the perfect graphene flakes in AB stacking and incommensurate stacking with different interlayer distances along different sliding directions [78].

the almost frictionless interface at the carbon-nanotube wall [80–82]. Because of the structural similarity, the extremely fast water transport through CNTs is also expected for graphene nanochannels. Some theoretical studies have been done on this subject. By considering equilibrium and nonequilibrium molecular dynamics simulations, Kannam et al. predicted a low friction coefficient between the fluids and graphene, indicating that water can be a good lubricant for graphene in shearing experiments and that graphene nanochannels can act as efficient water transport devices either for enhanced flow or for energy-saving flow [83, 84]. Furthermore, Xiong et al. showed that strain on graphene can drastically change the interfacial friction of water transport its nanochannel. Stretching the graphene walls increases the interfacial shear stress, whereas compressing the graphene walls reduces it. A detailed analysis of the molecular structure attributed this result to strain-induced change in the interfacial potential energy barrier and the commensurate structure between the graphene walls and the first water layer. In addition to theoretical works, a pioneering experiment done by N’guessan et al. probed water tribology on graphene [85]. They found that the lateral force required to slide a water drop on a graphene surface is independent of the resting time of the drop, contrary to classical experiments (Fig. 12). In addition, the drop’s three-phase contact line adopts a peculiar micrometric serrated form. This result was attributed to the absence of molecular reorientation on graphene with a chemically homogenous surface. Recently, Yin et al. showed that the droplets of ionic liquid can easily slide on a graphene surface [86] and, in a much more interesting result, they found that the movement of the liquid–solid–gas three-phase boundary on a graphene surface can generate electricity [86, 87]. All these results suggest that graphene is a promising material to construct efficient and intelligent channels for liquid flow.

4.6 Applications

Thanks to the advances in the fabrication of large-area 2D materials in quantity, especially graphene and *h*-BN, various promising applications that exploit the low adhesion and friction characteristics of these materials have been demonstrated. Kim et al.

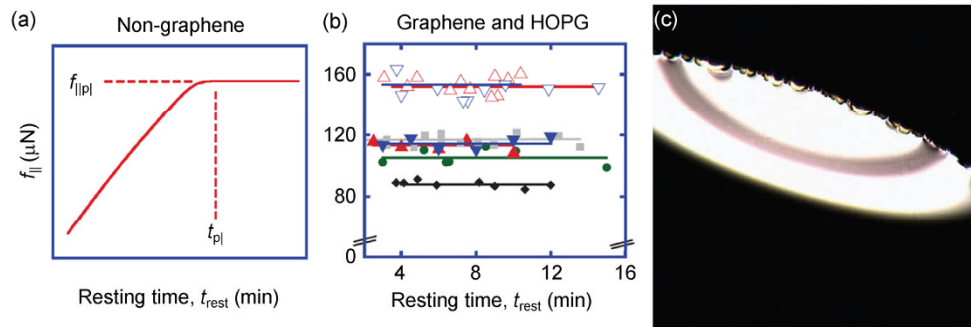


Fig. 12 Effect of time on drop retention force for various systems ((a) and (b)) and image of water drops on graphene (c) [85].

demonstrated that large-area graphene films prepared by chemical-vapor deposition reduces the adhesion and friction forces of the surface covered, contributed to the low surface energy, and multilayer graphene films with a few nanometers thick have coefficients of friction lower than that of bulk graphite [88]. In particular, graphene coatings can enhance the functionality of AFM probes, making them conductive and more resistance to wear [89]. Despite being covered by a low concentration of graphene flakes, the coefficient of friction can be reduced from 1 to 0.15 for 440C steel, and this coefficient persists for thousands of sliding passes, as demonstrated by Berman et al. [90]. For materials other than graphene, Li et al. demonstrated that *h*-BN prepared by chemical-vapor deposition can also reduce the friction of bare Cu by a factor of 40, even at a local pressure around 46 MPa [91]. This allows the *h*-BN domains to be easily distinguished from the copper substrate by FFM (Fig. 13).

Besides being useful for applications such as solid lubricants, flakes of 2D materials dispersed in water have also played a role in liquid lubricants. By adding oxide graphene nanosheets to pure water, Song et

al. improved the antiwear ability of a water-based lubricant and decreased the friction coefficient [92]. They proposed that the enhanced friction and wear arise from the formation of thin physical tribofilms of oxide graphene nanosheets on the substrate. They also demonstrated that adding even small amounts of *h*-BN nanosheets in water could enhance wear resistance and reduce the friction coefficient efficiently with good stability [93]. Tribofilms formed on worn surfaces due to repeated exfoliation and deposition of *h*-BN nanosheets during sliding, which is believed to be responsible for the tribological improvements with respect to aqueous dispersions. Accordingly, 2D materials, such as graphene and *h*-BN, offer the promise of being “green” lubricant additives for water.

When using 2D sheets as fillers, the frictional and antiwear properties of the composite may also be improved. Ren et al. demonstrated that the friction coefficients and wear rates for both graphene and polystyrene-functionalized-graphene-filled fabric-phenolic composites were reduced because of self-lubrication by graphene and the easily formed transfer film on the counterpart pin [94]. The wear rate of

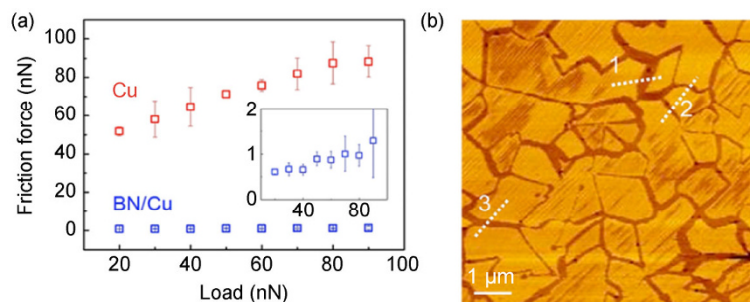


Fig. 13 Antifriction cover of monolayer *h*-BN [91].

PTFE is reduced by four orders of magnitude due to graphene additives according to a report by Kandanur et al. [95]. Graphene fillers were found to give 10 to 30 times lower wear rates than micrographite. These authors suggest that graphene additives are highly effective in regulating debris formation in PTFE, which results in reduced wear.

5 Summary

Low-dimensional materials and nanotechnology have given us chance to better understand the centuries-old phenomena of friction and to reduce friction and wear to a great degree from that of traditional materials and technology. Zero-dimensional nanoparticles can be applied in lubricants to reduce friction and wear. The interlayer friction in multiwalled nanotubes can be ultralow but is sensitive to the atomic lattice matching between the walls and interwall spacing, so ultralow-friction nanobearings and nanodevices may be designed and manufactured. Especially important are the two-dimensional nanomaterials such as graphene, *h*-BN, and transition-metal dichalcogenides, even the topological insulators. In contrast to the corresponding bulk materials, which serve as traditional dry lubricants, these high-quality monolayered materials grown in large sizes can serve as single-atom-thick coatings to reduce friction and wear, and their surface properties may be tuned efficiently. This type of ultralow friction coating with single-atom thickness promises a technological revolution by offering energy-efficient and/or self-powered electro-opto-magneto-mechanical nanosystems. In addition, the coating layer can also serve as a functional component in intelligent nanodevices. Because of the exceptionally low friction of such two-dimensional nanomaterials, friction-force microscopy can also serve as a powerful tool for characterizing their crystal quality. Therefore, friction research in low-dimensional materials calls for joint efforts with scientists from different disciplines.

Acknowledgments

This work was supported by The National Key Basic Research and Development (973) Program of China

(2013CB932604 and 2012CB933403), The National Natural Science Foundation of China (Nos. 51472117, 11072109, 11472131), the Research Fund of State Key Laboratory of Mechanics and Control of Mechanical Structures (0414K01, 0413G01, 0413Y02), the Jiangsu NSF (BK20131356, BK20130781), the Fundamental Research Funds for the Central Universities of China (No. NE2012005), and the Project Funded by the Priority Academic Program Development of Jiangsu Higher Education Institutions.

Open Access: This article is distributed under the terms of the Creative Commons Attribution License which permits any use, distribution, and reproduction in any medium, provided the original author(s) and source are credited.

References

- [1] Stachowiak G W, Batchelor A W. *Engineering Tribology (Tribology Series 24)*. Amsterdam: Elsevier, 1993: 539–562.
- [2] Holmberg K, Andersson P, Erdemir A. Global energy consumption due to friction in passenger cars. *Tribol Int* **47**: 221–234 (2012)
- [3] Meyer E, Overney R, Dransfeld K, Gyalog T. *Nanoscience: Friction and Rheology on the Nanometer Scale*. Singapore: World Scientific, 1998.
- [4] Dowson D. *History of Tribology*. London: Professional Engineering Publishing, 1998.
- [5] Bowden F P, Tabor D. *The Friction and Lubrication of Solids*. Oxford (UK): Oxford Univ Press, 1950.
- [6] Ruan J-A, Bhushan B. Atomic-scale friction measurements using friction force microscopy: Part I—General principles and new measurement techniques. *J Tribol* **116**: 378–388 (1994)
- [7] Bhushan B. Nanotribology and nanomechanics. *Wear* **259**: 1507–1531 (2005)
- [8] Tomlinson G. CVI. A molecular theory of friction. *Philos Mag* **7**: 905–939 (1929)
- [9] Kontorova T, Frenkel J. On the theory of plastic deformation and twinning. II. *Zh Eksp Teor Fiz* **8**: 1340–1348 (1938)
- [10] Weiss M, Elmer F-J. Dry friction in the Frenkel-Kontorova-Tomlinson model: Static properties. *Phys Rev B* **53**: 7539 (1996)
- [11] Matsushita K, Matsukawa H, Sasaki N. Atomic scale friction between clean graphite surfaces. *Solid State Commun* **136**: 51–55 (2005)
- [12] Bhushan B, Israelachvili J N, Landman U. Nanotribology:

- Friction, wear and lubrication at the atomic scale. *Nature* **374**: 607–616 (1995)
- [13] Guan Q F, Li G Y, Wang H Y, An J. Friction-wear characteristics of carbon fiber reinforced friction material. *J Mater Sci* **39**: 641–643 (2004)
- [14] Kim S J, Jang H. Friction and wear of friction materials containing two different phenolic resins reinforced with aramid pulp. *Tribol Int* **33**: 477–484 (2000)
- [15] Guo D, Xie G, Luo J. Mechanical properties of nanoparticles: Basics and applications. *J Phys D: Appl Phys* **47**: 013001 (2014)
- [16] Mate C, McClelland G, Erlandsson R, Chiang S. Atomic-scale friction of a tungsten tip on a graphite surface. *Phys Rev Lett* **59**: 1942–1945 (1987)
- [17] Dietzel D, Ritter C, Mönninghoff T, Fuchs H, Schirmeisen A, Schwarz U. Frictional duality observed during nanoparticle sliding. *Phys Rev Lett* **101**: 125505 (2008)
- [18] Tevet O, Von-Huth P, Popovitz-Biro R, Rosentsveig R, Wagner H D, Tenne R. Friction mechanism of individual multilayered nanoparticles. *Proceedings of the National Academy of Sciences* **108**: 19901–19906 (2011)
- [19] Park J Y, Ogletree D F, Salmeron M, Ribeiro R A, Canfield P C, Jenks C J, Thiel P A. High frictional anisotropy of periodic and aperiodic directions on a quasicrystal surface. *Science* **309**: 1354–1356 (2005)
- [20] Dietzel D, Feldmann M, Fuchs H, Schwarz U D, Schirmeisen A. Transition from static to kinetic friction of metallic nanoparticles. *Appl Phys Lett* **95**: 053104 (2009)
- [21] Xue Q, Liu W, Zhang Z. Friction and wear properties of a surface-modified TiO₂ nanoparticle as an additive in liquid paraffin. *Wear* **213**: 29–32 (1997)
- [22] Sawyer W G, Freudenberg K D, Bhimaraj P, Schadler L S. A study on the friction and wear behavior of PTFE filled with alumina nanoparticles. *Wear* **254**: 573–580 (2003)
- [23] Cizaire L, Vacher B, Le Mogne T, Martin J M, Rapoport L, Margolin A, Tenne R. Mechanisms of ultra-low friction by hollow inorganic fullerene-like MoS₂ nanoparticles. *Surf Coat Tech* **160**: 282–287 (2002)
- [24] Chhowalla M, Amaratunga G A J. Thin films of fullerene-like MoS₂ nanoparticles with ultra-low friction and wear. *Nature* **407**: 164–167 (2000)
- [25] Cumings J, Zettl A. Low-friction nanoscale linear bearing realized from multiwall carbon nanotubes. *Science* **289**: 602–604 (2000)
- [26] Cumings J, Collins P G, Zettl A. Materials: Peeling and sharpening multiwall nanotubes. *Nature* **406**: 586–586 (2000)
- [27] Fennimore A M, Yuzvinsky T D, Han W-Q, Fuhrer M S, Cumings J, Zettl A. Rotational actuators based on carbon nanotubes. *Nature* **424**: 408–410 (2003)
- [28] Zheng Q, Jiang Q. Multiwalled carbon nanotubes as gigahertz oscillators. *Phys Rev Lett* **88**: 045503 (2002)
- [29] Zheng Q, Liu J Z, Jiang Q. Excess van der Waals interaction energy of a multiwalled carbon nanotube with an extruded core and the induced core oscillation. *Phys Rev B* **65**: 245409 (2002)
- [30] Guo W, Guo Y, Gao H, Zheng Q, Zhong W. Energy dissipation in gigahertz oscillators from multiwalled carbon nanotubes. *Phys Rev Lett* **91**: 125501 (2003)
- [31] Zhao Y, Ma C-C, Chen G, Jiang Q. Energy dissipation mechanisms in carbon nanotube oscillators. *Phys Rev Lett* **91**: 175504 (2003)
- [32] Servantie J, Gaspard P. Methods of calculation of a friction coefficient: Application to nanotubes. *Phys Rev Lett* **91**: 185503 (2003)
- [33] Legoas S, Coluci V, Braga S, Coura P, Dantas S, Galvao D. Molecular-dynamics simulations of carbon nanotubes as gigahertz oscillators. *Phys Rev Lett* **90**: 055504 (2003)
- [34] Rivera J L, McCabe C, Cummings P T. Oscillatory behavior of double-walled nanotubes under extension: A simple nanoscale damped spring. *Nano Lett* **3**: 1001–1005 (2003)
- [35] Guo Z R, Chang T C, Guo X M, Gao H J. Thermal-Induced Edge Barriers and Forces in Interlayer Interaction of Concentric Carbon Nanotubes. *Phys Rev Lett* **107**: 105502 (2011)
- [36] Tangney P, Louie S G, Cohen M L. Dynamic sliding friction between concentric carbon nanotubes. *Phys Rev Lett* **93**: 065503 (2004)
- [37] Guo W, Gao H. Optimized bearing and interlayer friction in multiwalled carbon nanotubes. *Comput Model Eng Sci* **7**: 19–34 (2005)
- [38] Zhang R, Ning Z, Zhang Y, Zheng Q, Chen Q, Xie H, Zhang Q, Qian W, Wei F. Superlubricity in centimetres-long double-walled carbon nanotubes under ambient conditions. *Nat Nanotechnol* **8**: 912–916 (2013)
- [39] Urbakh M. Friction: Towards macroscale superlubricity. *Nat Nanotechnol* **8**: 893–894 (2013)
- [40] Guo W, Zhong W, Dai Y, Li S. Coupled defect-size effects on interlayer friction in multiwalled carbon nanotubes. *Phys Rev B* **72**: 075409 (2005)
- [41] Kis A, Jensen K, Aloni S, Mickelson W, Zettl A. Interlayer forces and ultralow sliding friction in multiwalled carbon nanotubes. *Phys Rev Lett* **97**: 025501 (2006)
- [42] Niguès A, Siria A, Vincent P, Poncharal P, Bocquet L. Ultrahigh interlayer friction in multiwalled boron nitride nanotubes. *Nat Mater* **13**: 688–693 (2014)
- [43] Polyakov B, Dorogin L M, Vlassov S, Kink I, Lohmus A, Romanov A E, Lohmus R. Real-time measurements of sliding friction and elastic properties of ZnO nanowires inside a scanning electron microscope. *Solid State Commun* **151**: 1244–1247 (2011)

- [44] Zhu Y, Qin Q, Gu Y, Wang Z. Friction and shear strength at the nanowire-substrate interfaces. *Nanoscale Res Lett* **5**: 291–295 (2009)
- [45] Conache G, Gray S M, Ribayrol A, Froberg L E, Samuelson L, Pettersson H, Montelius L. Friction measurements of InAs nanowires on silicon nitride by AFM manipulation. *Small* **5**: 203–207 (2009)
- [46] Kim H J, Kang K H, Kim D E. Sliding and rolling frictional behavior of a single ZnO nanowire during manipulation with an AFM. *Nanoscale* **5**: 6081–6087 (2013)
- [47] Qin Q, Zhu Y. Static friction between silicon nanowires and elastomeric substrates. *ACS Nano* **5**: 7404–7410 (2011)
- [48] Dorogin L M, Polyakov B, Petruhins A, Vlassov S, Löhmus R, Kink I, Romanov A E. Modeling of kinetic and static friction between an elastically bent nanowire and a flat surface. *J Mater Res* **27**: 580–585 (2012)
- [49] Novoselov K S, Geim A K, Morozov S V, Jiang D, Zhang Y, Dubonos S V, Grigorieva I V, Firsov A A. Electric field effect in atomically thin carbon films. *Science* **306**: 666–669 (2004)
- [50] Deacon R F, Goodman J F. lubrication by lamellar solid. *Proc R Soc Lond A, Mat Phys Sci* **243**: 464–482 (1958)
- [51] Chhowalla M, Amaratunga G A J. Thin films of fullerene-like MoS₂ nanoparticles with ultra-low friction and wear. *Nature* **407**: 164–167 (2000)
- [52] Hilton M R, Fleischauer P D. Applications of solid lubricant films in spacecraft. *Surf Coat Tech* **54–55**: 435–441 (1992)
- [53] Rowe G W. Some observations on the frictional behaviour of boron nitride and of graphite. *Wear* **3**: 274–285 (1960)
- [54] Lee H, Lee N, Seo Y, Eom J, Lee S. Comparison of frictional forces on graphene and graphite. *Nanotechnology* **20**: 325701 (2009)
- [55] Lee C, Wei X, Li Q, Carpick R, Kysar J W, Hone J. Elastic and frictional properties of graphene. *Physica Status Solidi (b)* **246**: 2562–2567 (2009)
- [56] Lee C, Li Q, Kalb W, Liu X Z, Berger H, Carpick R W, Hone J. Frictional characteristics of atomically thin sheets. *Science* **328**: 76–80 (2010)
- [57] Li Q, Lee C, Carpick R W, Hone J. Substrate effect on thickness-dependent friction on graphene. *Physica Status Solidi (b)* **247**: 2909–2914
- [58] Cho D-H, Wang L, Kim J S, Lee G H, Kim E S, Lee S, Lee S Y, Hone J, Lee C. Effect of surface morphology on friction of graphene on various substrates. *Nanoscale* **5**: 3063–3069 (2013)
- [59] Smolyanitsky A, Killgore J P, Tewary V K. Effect of elastic deformation on frictional properties of few-layer graphene. *Phys Rev B* **85**: 035412 (2012)
- [60] Ye Z, Tang C, Dong Y, Martini A. Role of wrinkle height in friction variation with number of graphene layers. *J Appl Phys* **112**: 116102 (2012)
- [61] Barboza A P M, Chacham H, Oliveira C K, Fernandes T F D, Ferreira E H M, Archanjo B S, Batista R J C, de Oliveira A B, Neves B R A. Dynamic negative compressibility of few-layer graphene, h-BN, and MoS₂. *Nano Lett* **12**: 2313–2317 (2012)
- [62] Egberts P, Han G H, Liu X Z, Johnson A T C, Carpick R W. Frictional behavior of atomically-thin sheets hexagonal-shaped graphene islands grown on copper by chemical vapor deposition. *ACS Nano* **8**: 5010–5021 (2014)
- [63] Filletter T, McChesney J, Bostwick A, Rotenberg E, Emtsev K, Seyller T, Horn K, Bennewitz R. Friction and dissipation in epitaxial graphene films. *Phys Rev Lett* **102**: 086102 (2009)
- [64] Filletter T, Bennewitz R. Structural and frictional properties of graphene films on SiC(0001) studied by atomic force microscopy. *Phys Rev B* **81**: 155412 (2010)
- [65] Byun I S, Yoon D, Choi J S, Hwang I, Lee D H, Lee M J, Kawai T, Son Y W, Jia Q, Cheong H, Park B H. Nanoscale lithography on monolayer graphene using hydrogenation and oxidation. *ACS Nano* **5**: 6417–6424 (2011)
- [66] Shin Y J, Stromberg R, Nay R, Huang H, Wee A T S, Yang H, Bhatia C S. Frictional characteristics of exfoliated and epitaxial graphene. *Carbon* **49**: 4070–4073 (2011)
- [67] Pandey D, Reifengerger R, Piner R. Scanning probe microscopy study of exfoliated oxidized graphene sheets. *Surf Sci* **602**: 1607–1613 (2008)
- [68] Zhang J, Lu W, Tour J M, Lou J. Nanoscale frictional characteristics of graphene nanoribbons. *Appl Phys Lett* **101**: 123104 (2012)
- [69] Wang L F, Ma T B, Hu Y Z, Wang H. Atomic-scale friction in graphene oxide: An interfacial interaction perspective from first-principles calculations. *Phys Rev B* **86**: 125436 (2012)
- [70] Deng Z, Smolyanitsky A, Li Q, Feng X Q, Cannara R J. Adhesion-dependent negative friction coefficient on chemically modified graphite at the nanoscale. *Nat Mater* **11**: 1032–1037 (2012)
- [71] Fessler G, Eren B, Gysin U, Glatzel T, Meyer E. Friction force microscopy studies on SiO₂ supported pristine and hydrogenated graphene. *Appl Phys Lett* **104**: 041910 (2014)
- [72] Kwon S, Ko J H, Jeon K J, Kim Y H, Park J Y. Enhanced nanoscale friction on fluorinated graphene. *Nano Lett* **12**: 6043–6048 (2012)
- [73] Hölscher H, Ebeling D, Schwarz U D. Friction at atomic-scale surface steps: Experiment and theory. *Phys Rev Lett* **101**: 246105 (2008)
- [74] Liu P, Zhang Y W. A theoretical analysis of frictional and defect characteristics of graphene probed by a capped single-walled carbon nanotube. *Carbon* **49**: 3687–3697 (2011)
- [75] Kwon S, Choi S, Chung H J, Yang H, Seo S, Jhi S H, Young Park J. Probing nanoscale conductance of monolayer graphene under pressure. *Appl Phys Lett* **99**: 013110 (2011)

- [76] Choi J S, Kim J S, Byun I S, Lee D H, Lee M J, Park B H, Lee C, Yoon D, Cheong H, Lee K H, Son Y W, Park J Y, Salmeron M. Friction anisotropy-driven domain imaging on exfoliated monolayer graphene. *Science* **333**: 607–610 (2011)
- [77] Verhoeven G S, Dienwiebel M, Frenken J W. Model calculations of superlubricity of graphite. *Phys Rev B* **70**: 165418 (2004)
- [78] Guo Y, Guo W, Chen C. Modifying atomic-scale friction between two graphene sheets: A molecular-force-field study. *Phys Rev B* **76**: 155429 (2007)
- [79] Bonelli F, Manini N, Cadelano E, Colombo L. Atomistic simulations of the sliding friction of graphene flakes. *Eur Phys J B* **70**: 449–459 (2009)
- [80] Whitby M, Quirke N. Fluid flow in carbon nanotubes and nanopipes. *Nat Nano* **2**: 87–94 (2007)
- [81] Majumder M, Chopra N, Andrews R, Hinds B J. Nanoscale hydrodynamics: Enhanced flow in carbon nanotubes. *Nature* **438**: 44 (2005)
- [82] Holt J K, Park H G, Wang Y, Stadermann M, Artyukhin A B, Grigoropoulos C P, Noy A, Bakajin O. Fast mass transport through sub-2-nanometer carbon nanotubes. *Science* **312**: 1034–1037 (2006)
- [83] Kannam S K, Todd B D, Hansen J S, Daivis P J. Slip length of water on graphene: Limitations of non-equilibrium molecular dynamics simulations. *J Chem Phys* **136**: 024705 (2012)
- [84] Kannam S K, Todd B D, Hansen J S, Daivis P J. Slip flow in graphene nanochannels. *J Chem Phys* **135**: 114701 (2011)
- [85] N'guessan H E, Leh A, Cox P, Bahadur P, Tadmor R, Patra P, Vajtai R, Ajayan P M, Wasnik P. Water tribology on graphene. *Nat Commun* **3**: 1242 (2012)
- [86] Yin J, Li X, Yu J, Zhang Z, Zhou J, Guo W. Generating electricity by moving a droplet of ionic liquid along graphene. *Nat Nano* **9**: 378–383 (2014)
- [87] Yin J, Zhang Z, Li X, Yu J, Zhou J, Chen Y, Guo W. Waving potential in graphene. *Nat Commun* **5**: 3582 (2014)
- [88] Kim K-S, Lee H-J, Lee C, Lee S-K, Jang H, Ahn J-H, Kim J-H, Lee H-J. Chemical vapor deposition-grown graphene: The thinnest solid lubricant. *ACS Nano* **5**: 5107–5114 (2011)
- [89] Martin-Olmos C, Rasool H I, Weiller B H, Gimzewski J K. Graphene MEMS: AFM probe performance improvement. *ACS Nano* **7**: 4164–4170 (2013)
- [90] Berman D, Erdemir A, Sumant A V. Reduced wear and friction enabled by graphene layers on sliding steel surfaces in dry nitrogen. *Carbon* **59**: 167–175 (2013)
- [91] Li X, Yin J, Zhou J, Guo W. Large area hexagonal boron nitride monolayer as efficient atomically thick insulating coating against friction and oxidation. *Nanotechnology* **25**: 105701 (2014)
- [92] Song H-J, Li N. Frictional behavior of oxide graphene nanosheets as water-base lubricant additive. *Appl Phys A* **105**: 827–832 (2011)
- [93] Cho D H, Kim J S, Kwon S H, Lee C, Lee Y Z. Evaluation of hexagonal boron nitride nano-sheets as a lubricant additive in water. *Wear* **302**: 981–986 (2013)
- [94] Ren G, Zhang Z, Zhu X, Ge B, Guo F, Men X, Liu W. Influence of functional graphene as filler on the tribological behaviors of Nomex fabric/phenolic composite. *Compos Part A: Appl Sci Manuf* **49**: 157–164 (2013)
- [95] Kandanur S S, Rafiee M A, Yavari F, Schrameyer M, Yu Z-Z, Blanchet T A, Koratkar N. Suppression of wear in graphene polymer composites. *Carbon* **50**: 3178–3183 (2012)



Wanlin GUO. He obtained his bachelor, master and PhD degrees in solids mechanics in 1985, 1988, and 1991 respectively from Northwestern polytechnical University, Xi'an, China. From 1991 he has worked as Post-D, associated professor and professor

in Xi'an Jiaotong University. From 1995 to 1998, he worked at the Center-of-Expertise of Australian Defence Science and Technology Organization at Monash University. He worked as Chair Professor Position of the Education Ministry of China in

Nanjing University of Aeronautics and Astronautics since 2000. Prof. Wanlin Guo obtained the Outstanding Young Scientist Award (Premier Fund) of China in 1996 and the honor of Cheung Kong Scholars in 1999. In 2012, he was awarded the 2nd National Prize in Nature Science for his contribution to nanomechanics. His current research interests cover nanoscale physical mechanics, intelligent nano materials and devices, high efficient energy transfer nanotechnology, and three dimensional fatigue fracture and damage tolerance and durability design of structures.